



ISSN: 2579-1184(Print)

ISSN: 2578-1129 (Online)

<http://fupre.edu.ng/journal>

## Synthesis and characterization of copper doped TiO<sub>2</sub> via electrodeposition method for photovoltaic applications

IJEH, R. O.<sup>1\*</sup> , IMOSOBOMEH, L. I.<sup>2</sup> , EZEMA, F. I.<sup>2</sup>

<sup>1</sup>Department of Physics, University of Delta, Agbor, Nigeria

<sup>2</sup>Department of Physics and Astronomy, University of Nigeria Nsukka, Nigeria

### ABSTRACT

#### ARTICLE INFO

Received: 10/07/2024  
Accepted: 21/10/2024

#### Keywords

Electrodeposition,  
Doping, Nanoparticles,  
Titanium dioxide

Indium doped Tin Oxide (ITO) substrate was used to synthesize Cu and Cu-TiO<sub>2</sub> nanocrystals via electrochemical deposition method. The techniques used for analyzing the structure, morphology, optical, magnetic and electrical properties include X-ray diffractometry, scanning electron microscopy, energy dispersive X-ray (EDAX), UV-visible spectrophotometer, It was discovered that the energy bandgap shrank from 3.3 - 3.1 eV. The magnetic analysis showed a characteristic ferromagnetic ordering, with  $5.13 \times 10^{-4}$  emu/g for the 3% and  $6.08 \times 10^{-4}$  emu/g for the 5% samples, respectively. The maximum conductivity of  $0.08 \Omega\text{cm}^{-1}$  was recorded by the 5% doped thin film.

## 1. INTRODUCTION

Titanium dioxide (TiO<sub>2</sub>) is a transparent conducting oxide which belongs to group II–VI semiconductor material. TiO<sub>2</sub> has a wide bandgap ( $E_g \geq 3$  eV) and high refractive index which makes it potent in the field of science and industries Zeribi et al., (2022), Kim et al., (2015) and Tipparak, et al., (2017). Naturally TiO<sub>2</sub> has high resistivity value near  $10^8 \Omega\text{cm}$  and with excess titanium ions ultimately alters the stoichiometric composition which results to n-type semiconductor. According to Mariatz et al., (2017) the distortion of the crystal arising from the change in composition of oxygen to titanium ratio

culminates into enhancement of its electrical properties TiO<sub>2</sub> thin film has attracted attention of researchers for some decades due to the physical, electrical and chemical properties which has enhanced its applications for photonic device and solar cell, photo-catalysis, gas sensing, optical filters and anti-reflection coatings (Haque et al., 2019). The photoactivity property of TiO<sub>2</sub> is well exhibited by the anatase and rutile polymorphs under solar light irradiation according to Comert et al., (2016). It has also been recorded amongst researchers that TiO<sub>2</sub> has high recombination rate of electron hole pairs and absorbs ultra violet light in low

\*Corresponding author, e-mail:rufus.ijeh@unidel.edu.ng

DIO

©Scientific Information, Documentation and Publishing Office at FUPRE Journal

wavelength region. However, the utmost performance of TiO<sub>2</sub> can be obtained by structural modification in terms of doping with transition metals (Tipparak et al., 2017). It is obvious that copper has a high absorption coefficient with relatively narrow band gap which easily reduces the bandgap of the host atom (karabulut et al., 2018). Copper dopant in titanium lattice enhances electrical conductivity by reducing electron recombination and having a similar ionic radius to titanium (Thangama et al., 2017, Khan et al., 2017). It is certain that dopants such as cobalt, chromium, nickel, iron, etc have been used to dope titanium oxide adopting several deposition techniques. The work centered on doping of TiO<sub>2</sub> with copper using electrodeposition method in order to study the optical, electrical and magnetic properties as work done by other researchers were limited to the optical properties of TiO<sub>2</sub> using other methods of deposition. The electrodeposition method was preferred amongst other methods due to its cost effectiveness, simplicity, environmental friendliness (Bensouici et al., 2016). Many deposition techniques that have been employed for the doping of copper on titanium thin films include sol-gel (Dharmadasaz and Haigh, 2006), Spray pyrolysis (Khan et al., 2017), Hydrothermal (Patel and Gajbhiye, 2012), Chemical Vapour Deposition (Fasakin et al., 2013). Furthermore, Perarasan et al., (2019) adopted chemical hydrolysis technique to synthesize Cu doped titanium dioxide nanoparticles. The XRD technique revealed tetragonal structure with anatase phase and the SEM results depicted nanoparticles of spherical morphology. The optical absorbance showed increase of bandgap with percentage doping. The optical properties of Cu-TiO<sub>2</sub> was studied by Álvaro et al., (2017) using green synthesis technique. The spherical shape of the particles and their average size of 27.3 to 70 nm were revealed through SEM imaging.

As the amount of Cu increased, the band gap energy showed a reduction. Ahmed et al., (2017) used the inert gas condensation technique to analyze the structural and optical properties of Cu-TiO<sub>2</sub>. The XRD patterns clearly indicated the presence of rutile phase peaks in both the undoped and Cu-doped TiO<sub>2</sub> thin films. As copper concentration increased, the energy band gaps showed a decrease. Also Khan et al., (2017) used sol-gel spin coating method to investigate the electrical properties of Cu doped TiO<sub>2</sub>. The morphology of the thin films showed that the number of layers increased proportionately with the grain size and the resistivity decreased with increasing layer. TiO<sub>2</sub> is a valuable material that absorbs photons and readily converts them into electric current and high value of transmittance of titanium dioxide makes it suitable for photovoltaic applications as window layer.

## 2. Experimental Procedure

### 2.1 Materials

The substrate used is indium-doped tin oxide., sodium hydroxide, titanium trichloride (TiCl<sub>3</sub>) citric acid as buffer, copper sulphate pentahydrate solution (CuSO<sub>4</sub>.5H<sub>2</sub>O) and, in the process of electrochemical deposition for undoped and Cu-TiO<sub>2</sub> films, silver monochloride electrodes were used.

### 2.2. Synthesis

Electrodeposition was utilized to produce Cu-TiO<sub>2</sub> and undoped TiO<sub>2</sub> thin films. To ensure strong adhesion to the ITO and promote material growth, the ITO coated substrates were cleaned with detergent, rinsed, and exposed to acetone for 30 minutes. Then 100 ml of 0.5 M titanium trichloride (TiCl<sub>3</sub>) was mixed with 3% and 5% weight of CuSO<sub>4</sub>.5H<sub>2</sub>O solution at room temperature to prepare the solutions of the undoped TiO<sub>2</sub> and 60 ml of 1 mol of NaOH was mixed with 100 ml of TiCl<sub>3</sub>. For each of

the depositions, an ITO-coated substrate was positioned upright in a three-electrode chamber that contained the anode, working electrode, and reference electrode. On the other hand, the deposition was done for 5 minutes at a potentiostatic state of -200 mV. Following the completion of deposition, both undoped and Cu-TiO<sub>2</sub> thin films were subjected to cleaning, drying, and annealing at 300°C for 30 minutes.

### 2.3 Characterization

Figure 1 illustrates the diffraction patterns of both undoped TiO<sub>2</sub> and Cu-TiO<sub>2</sub> films. Philips diffractometer model PW1800 was used to characterize the XRD patterns of the annealed films, revealing crystallographic phases between 10°C ≤ 2θ ≤ 70°C. The films' surface micrograph was examined using a JEOL JSM 35 CF SEM, and the copper doped films' elemental composition was analyzed with EDAX. The JASCO 670, a double beam UV-Vis, NIR spectrophotometer, was utilized to analyze optical properties between 300 and 1000 nm in wavelength. Using a VSM (Lake Shore Model 7404), the magnetization data was collected, while the resistivity of the thin films was measured using a Keithley 182 Nanovoltmeter.

## 3. Result and discussions

### 3.1. Phase studies

Fig. 1 displays the diffraction patterns of undoped and copper-doped TiO<sub>2</sub> films. The observed pattern of several peaks diffracted at 29.35°, 33.94°, 35.11°, 50.12° and 65.58° which confirmed anatase phase assigned to (101), (110), (220), (022), (123) crystal planes respectively. The peaks are of polycrystalline phase with high intensity peaks for the doped samples at (101), 110, (220), (022), (123) orientation which agrees with JCPDS file. There is little difference in diffraction patterns between the undoped and doped samples. This might be due to the small concentration of Cu<sup>+2</sup> that dissolved

into TiO<sub>2</sub> crystal lattice having almost same ionic radii. The works of Perarasan et al., (2019) and Sokoidanto et al., (2020) also confirmed anatase phase resulting to increase in crystallite sizes of TiO<sub>2</sub> when doped with copper. The average crystallite sizes of the undoped and doped films were calculated using Scherer equation as shown in equation.

$$D = \frac{k\lambda}{\beta \cos\theta}$$

(1)

The variables in equation 1 are defined as follows: λ is X-ray wavelength, d is crystallite size, θ is diffraction angle, and β is full width of half maximum.

### 3.2 Surface micrograph of the material

The surface morphologies of undoped and copper doped titanium dioxide films generated at room temperature is as illustrated in Figure 2.1(a-c). There is agglomeration of cross-linked, grey and irregular spherical nanostructures in the 5% doped sample than the 3% doped and the undoped. The undoped sample is denser than the 3% and 5% doped samples as illustrated in Figure 2. (a). The effect of doping is more pronounced in the 5% doped sample than the 3% doped and undoped thin films. This indicates the presence of copper in the lattice crystals of titanium dioxide. This same result that showed increase in doping percentage without cracks was also obtained by Zhang et al., (2004) and Natsir et al., (2021). The EDAX images depicted in Fig. 2 (a-c) depicts the characteristic peaks of Ti, O and Cu elements. The EDX analysis performed was to find out the percentage of the elemental constituents arising from the synthesis. The characterization result showed the peak of Ti at 2.0 KeV, the peak of O at 0.31 KeV and the peak of Cu at 2.5 KeV as shown in Fig. 2. (a-c).

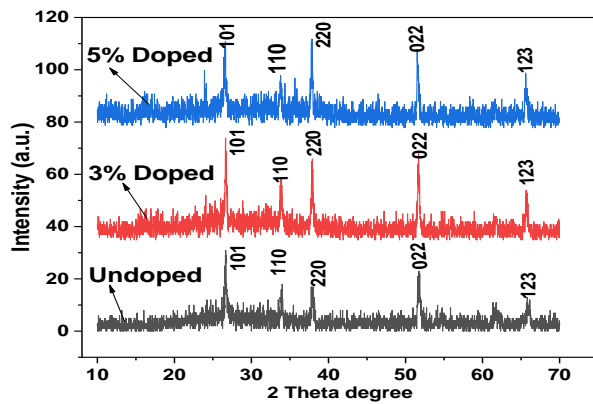


**Fig. 1.** XRD of TiO<sub>2</sub> for the undoped and doped samples

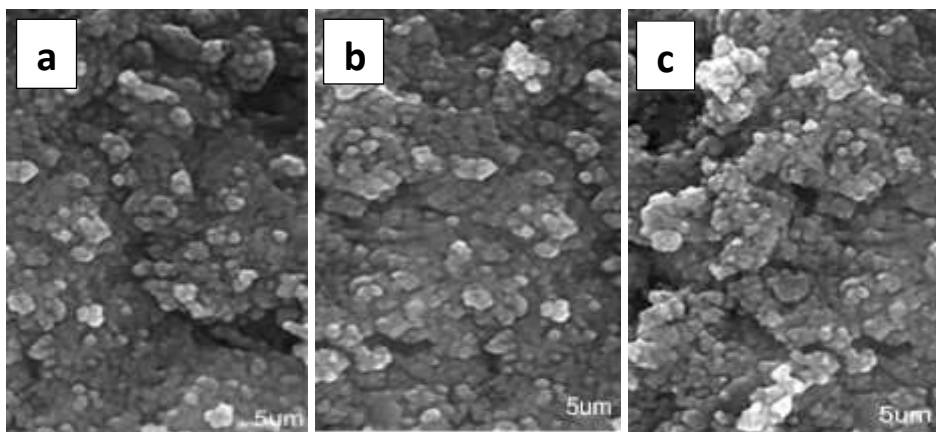


**Fig. 2.** SEM images of (a) undoped TiO<sub>2</sub>, (b) 3% Cu:TiO<sub>2</sub> and (c) 5% Cu:TiO<sub>2</sub>

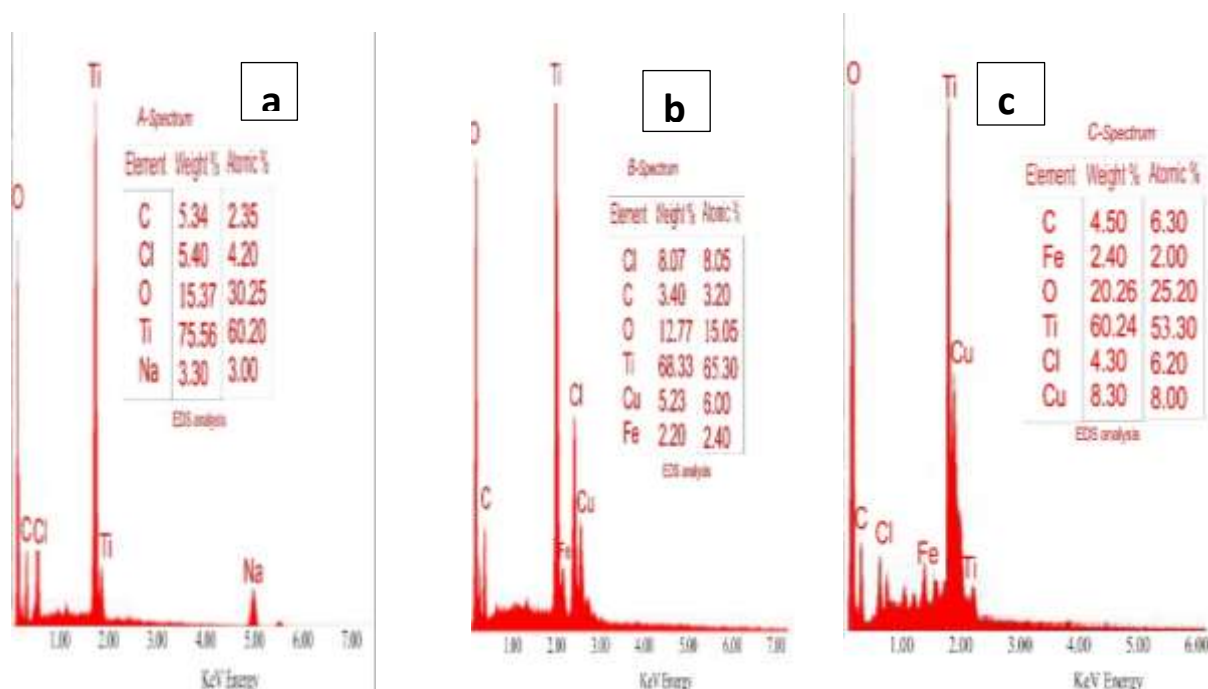


**Fig. 3.** EDAX spectra of (a) undoped TiO<sub>2</sub>, (b) 3% Cu:TiO<sub>2</sub> and (c) 5% Cu:TiO<sub>2</sub>

### 3.3 Optical studies

Figure 4 (a & b) displays absorbance and transmittance spectra in the 300-1000 nm optical range at room temperature. By employing a UV-visible spectrophotometer, we were able to quantify the absorbance and transmittance. Both undoped and doped films show a decrease in absorbance as the wavelength increases in the visible region. At a wavelength of 450 nm, the 5% doped thin film exhibited an absorption of 33.6%, while the 3% and undoped thin films had absorptions of 31.5% and 28.2% respectively, as depicted in Fig. 3a. This result is in accordance with the works of Ahmed et. al., (2017). It is observable that within the wavelength range of 450nm to 800nm, the transmittance spectra showed that the undoped and 3% doped thin films transmitted highest values of 56% to 83%. This result is attuned with the works of Khan et al., (2017).

### 3.4 Optical band gap

The plot of absorption coefficient versus photons energy as shown in Fig.5 is used to

determine the optical band gaps of the undoped and Cu-doped thin films. The optical bandgaps were calculated using Taucs relation as shown in equation (2).

$$(\alpha h\nu)^2 = A(h\nu - E_g)^n \quad (2)$$

The absorption coefficient  $A$  depicts the constant that relies on the photon energy  $h\nu$  and the band gap energy  $E_g$ . As depicted in Fig. 5, the energy band gap decreases with an increase in doping percentage. Copper has the ability to modify the absorption properties of titanium by absorbing visible light and introducing electron states to the lattice structure. A change in local levels density causes a decrease in optical energy gap values. The decrease in energy bandgap values may be a result of the increase in grain size. In the undoped TiO<sub>2</sub> thin film, the direct band gaps were determined to be 3.32 eV, whereas the 3% and 5% doped films displayed bandgaps of 3.18 and 3.10 eV, respectively. This result is in concordant with the works of Suber et al., (2021) and Bedikyan et al., (2013). Also Heiba et al.,

(2022) worked on copper doped titanium dioxide and got the bandgap energy values that ranged from 3.18 to 3.38 eV for higher

doping percentage of 5-10% while Natsir et al., (2021) calculated the band gap of copper doped titanium dioxide as 3.10 eV .

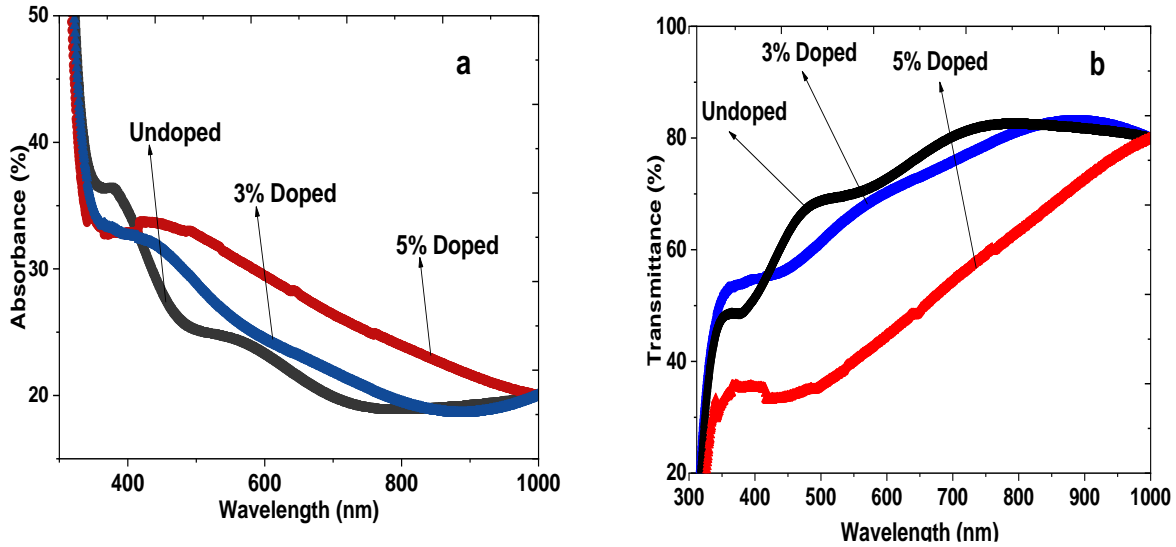


Fig. 4. [a] Absorbance and [b] Transmittance spectra for the undoped and doped TiO<sub>2</sub>: Cu films

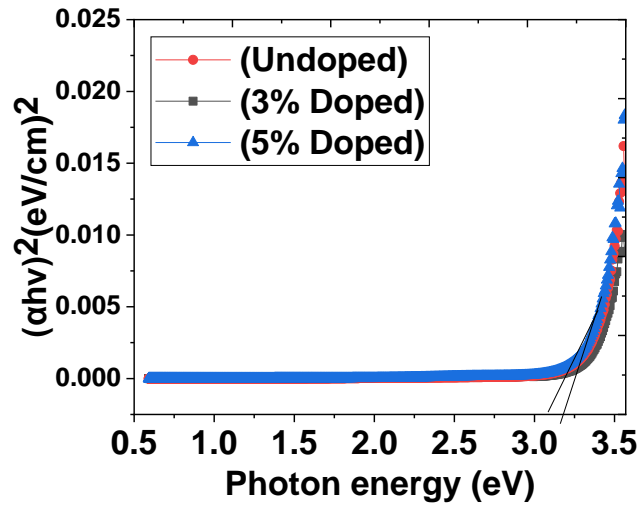


Fig. 5. Plot of bandgaps of the materials.

### 3.5. Refractive index

Refractive index

The refractive indices for the doped and Cu:TiO<sub>2</sub> were obtained using equation (3) [31]:

$$\eta = (1 + \sqrt{R}) / (1 - \sqrt{R}) \tag{3}$$

The refractive index is represented by  $\eta$ , and reflectance is denoted by R. Figure 6 illustrates the relationship between photon energy and refractive index for undoped and Cu-TiO<sub>2</sub> thin films. Fig 6 shows that the refractive index values rose at low wavelengths and reached a peak of 1.6 for the undoped sample, while the 3% and 5% thin

films peaked at 1.5 and 1.3 respectively. It was observed that at low photon energy, the highest value for undoped film is 2.1 while the maximum values for 3% and 5% doped thin films are 1.8 and 1.7 respectively. The refractive indices of the films ranged from 2.54 to 2.64 as the wavelength increased. The result is in accordant with the works of Horzuma et al., (2019) that used sol-gel dip coating had refractive indices values ranged from 2.05 to 3.26. But at higher photon energy, the 5% doped increased gradually to 2.4 while both the 3% and undoped thin films peaked at 2.1. This suggests that the

refractive index increases with doping. This increase is due to annihilation of holes as the film surface becomes denser with increase in doping level. The 3% and undoped thin films maintained the same value due to imperfections of crystals. Furthermore, the denser material has a larger refractive index since more electric dipoles are triggered due to the electric field of the light radiation. The works of Vidhya et al., (2016) showed a calculated value of refractive index of Cu doped Titanium dioxide thin film annealed at 400 °C as 2.7.

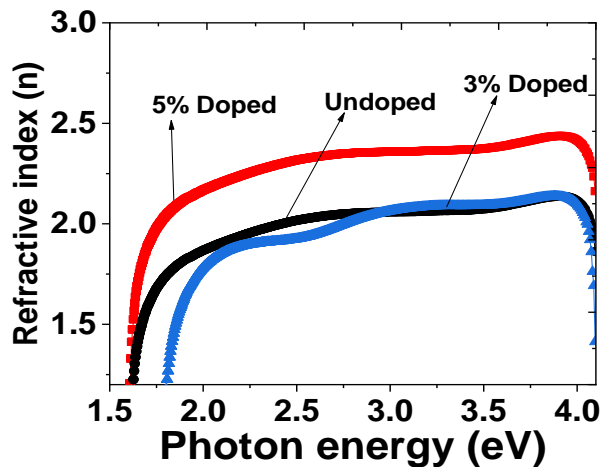


**Fig. 6.** Plot of refractive index of the films

### 3.6. Extinction Coefficient

Figure 7 compares both undoped and Cu:TiO<sub>2</sub> to show how the extinction coefficient changes with photon energy. The 3% and undoped samples exhibit a high level of transparency as their extinction coefficient

approaches negative values at very low photon energy. However, the 5% doped sample initially increases rapidly and later decreases compared to the 3% and undoped films.

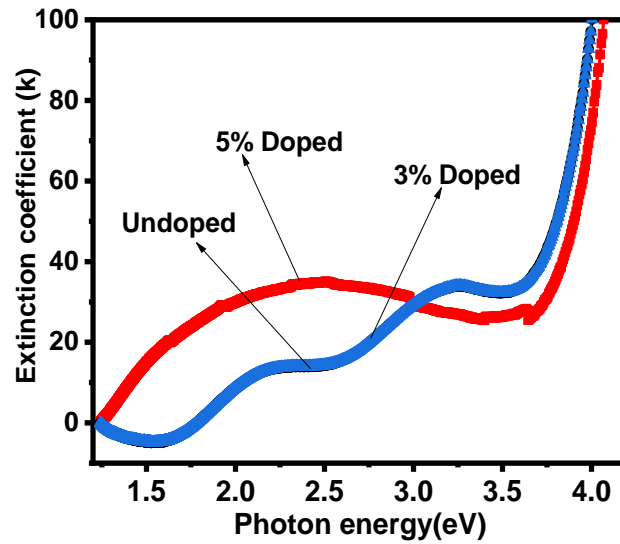


**Fig. 7.** Plot of Extinction coefficient of the undoped and doped TiO<sub>2</sub> thin films

### 3.7. Dielectric constant

By analyzing equations 3 and 4, we can gain significant insights into the dielectric constants of materials and their impact on refractive index, absorption, and extinction coefficient.

$$\epsilon_r = n^2 - k^2 \quad (3)$$

$$\epsilon_i = 2nk \quad (4)$$

The refractive index is denoted by  $n$  and the extinction coefficient is denoted by  $k$ .

Real part of dielectric constant measures the attenuation of intensity of light occasioned by scattering and absorption while the imaginary part connotes the energy dissipation to the medium. Figure 8 (a & b) illustrates the real and imaginary components of the dielectric constants. An inverse relationship was observed between photon energy and both the real and imaginary parts of the dielectric constant. The imaginary section has a larger proportion of negative values than the real section.



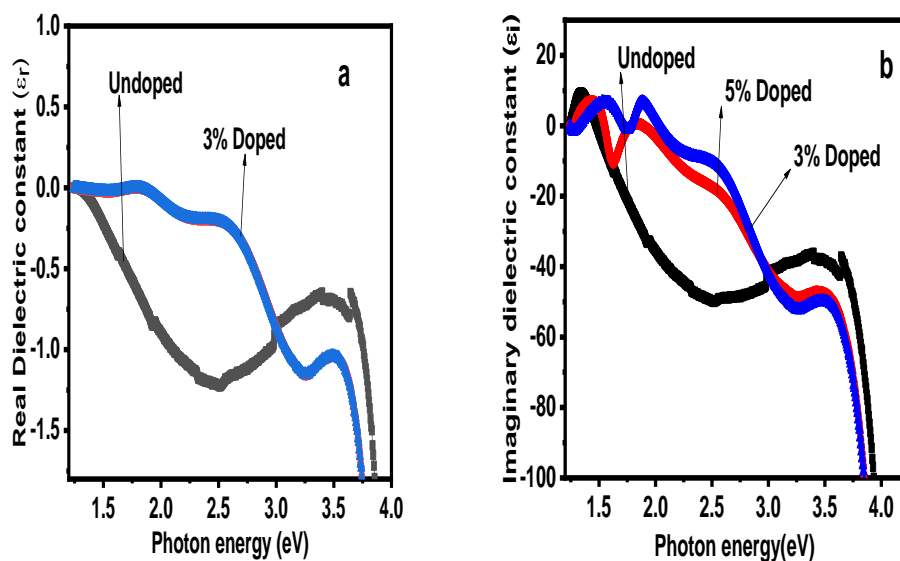


**Fig. 8.** Plot of Dielectric constants [a] real and [b] imaginary of the films

### 3.8. Magnetic studies of TiO<sub>2</sub> thin films

Magnetic investigations of undoped and copper doped TiO<sub>2</sub> films were carried out using the VSM technique in a conducted study. The plotted magnetic characteristics curves in Fig 6 illustrate the magnetic moment's dependence on the applied magnetic field (M-H). The behavior of magnetism in undoped and copper-doped TiO<sub>2</sub> films shows how the magnetic field impacts the samples visually. The presence of copper doping in TiO<sub>2</sub> thin films demonstrates a connection between electron transfer and magnetic exchange interactions. The M-H loop reveals that both undoped TiO<sub>2</sub> and the doped samples exhibited ferromagnetic behavior, as depicted in Fig. The undoped sample has a saturation magnetization of around  $4.18 \times 10^{-4}$  (emu/g), a coercivity of 43.25, and a squareness value

of 0.054. When TiO<sub>2</sub> is doped with 3% copper, the magnetization increases to  $5.13 \times 10^{-4}$  (emu/g) and the squareness value increases to 0.057. When doped with 5% copper, the magnetization and squareness value increased to  $6.08 \times 10^{-4}$  (emu/g) and 0.064, respectively, indicating the doping effect. The doped samples' squareness values are less than 0.5, indicating that the inserted copper has not fully coupled with the titanium atom. The result is in agreement with the works of Ijeh et al., (2022). The low remnant values of all the samples lie between (0.0000229 - 0.0000393) emu/g. The M-H loop provides evidence of increased magnetization, potentially caused by the presence of oxygen vacancies. Table 1 displays the values of  $M_s$ ,  $M_r$ ,  $H_c$ , and the squareness ratio.

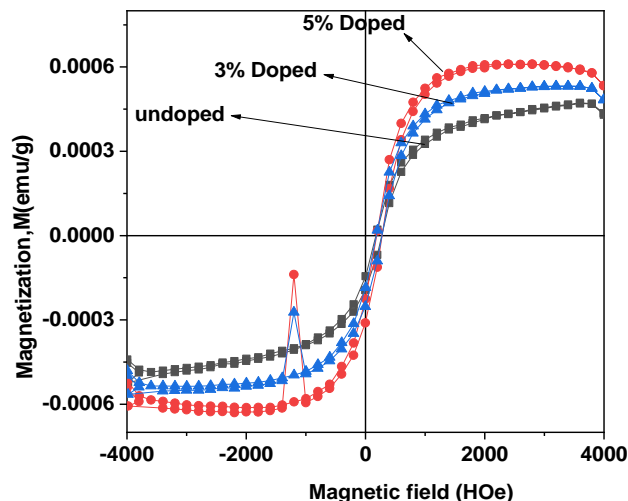


Fig. 7. Magnetic curves of the films.

**Table 1: Magnetization of films**

Sample	Magnetic saturation ( $M_s$ ) (emu/g)	Remnant magnetization ( $M_r$ ) (emu/g)	Coercive field ( $H_c$ ) ( $O_e$ )	Squareness Value
Undoped	$4.18 \times 10^{-4}$	$2.29 \times 10^{-5}$	43.25	0.054
3% Doped	$5.13 \times 10^{-4}$	$2.93 \times 10^{-5}$	45.32	0.057
5% Doped	$6.08 \times 10^{-4}$	$3.93 \times 10^{-5}$	48.39	0.064

### 3.9. Electrical studies of the films

To assess the resistivity of titanium dioxide, a four-point probe was utilized to measure the resistance encountered by charge carriers. The study in Figure 8 demonstrates the relationship between electrical conductivity ( $\sigma$ ) and doping percentage in both pure and Cu-TiO<sub>2</sub> films at ambient temperature. The conductivity values of the 5% and 3% doped samples demonstrate a noticeable rise in comparison. Adding Cu to titanium crystal enhanced the conducting abilities of the samples without impacting their fundamental traits, as the findings imply.

Figure 8 displays the exploration of the impact of doping percentage on the electrical conductivity ( $\sigma$ ) of undoped and Cu-TiO<sub>2</sub> films at ambient temperature. The 5% doped sample exhibits a significant increase in conductivity value compared to the 3% doped sample. The conductivity of the TiO<sub>2</sub> sample improved with the addition of Cu into the titanium crystal, as indicated by the results. It was observed that for the 3% and 5% doped films, there was evidence of sharp increase in conductivity to  $0.03 \Omega\text{cm}^{-1}$  and  $0.07 \Omega\text{cm}^{-1}$  respectively while the undoped film was 0% as it was devoid of carrier

density. Also the works of Ijeh et al., (2020) showed that the conductivity for copper doped  $\text{MoO}_3$  varies from  $1.0$  to  $1.5 \Omega\text{cm}^{-1}$ .

The higher doping percentage results in a greater concentration of carriers, leading to an increase in electrical conductivity.

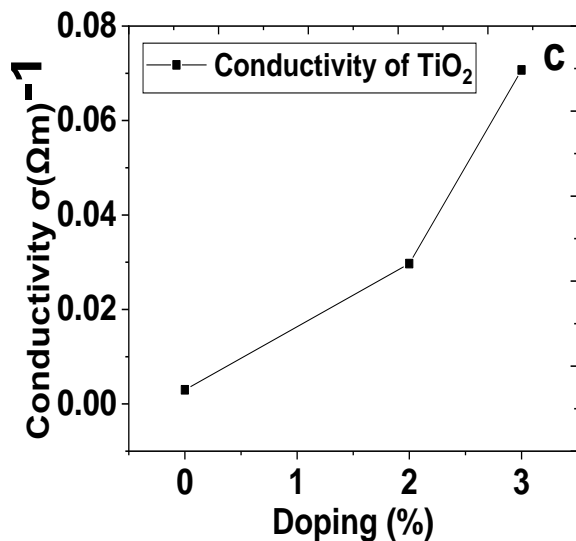


**Fig. 8.** Electrical conductivity versus doping of  $\text{TiO}_2$  thin films

#### 4. CONCLUSION

The crystallite showed only anatase phase structure and the surface morphology of the films indicated the influence of copper doping on titanium dioxide. The energy bandgap decreased slightly with increase in doping. The result of FTIR revealed functional group bonds which validated Cu-doped  $\text{TiO}_2$ . The incorporation of titanium in  $\text{Cu}_2\text{O}$  leads to thrilling advances in optical improvements. Characteristics of films of  $\text{Cu}_2\text{O}$  regarding their magnetic and electrical properties. This research work is genuine for photovoltaic applications and optoelectronic devices.

#### References

Ahmed, H. A., Abu-Eishah, S. I., Ayesh, A. I., and Mahmoud, S. T (2017). Synthesis and characterization of Cu-doped  $\text{TiO}_2$  thin films produced by the inert gas

condensation technique *Journal of Physics: Conference Series*, 869, (2017) 012027.

doi:10.1088/1742- 596/869/1/012027.

Alvaro, R. J., Diana, N. D., Maria, A. M (2017). Effect of Cu on optical properties of  $\text{TiO}_2$  nanoparticle *Contemporary Engineering Sciences* 10, 31, 1539-1549.

Bedikyan, L., Zakhariyev, S., Zakhariyeva, M (2013). Titanium dioxide thin films: Preparation and Optical properties, *Journal of Chemical Technology and Metallurgy* 48, 6, 555-558.

Bensouici, F., Bououdina, M., Dakhel, A.A., Tala-Ighil, R., Tounane, M., Iratni, A., Souier, T., Liu, S., and Cai, W (2016). Optical, Structural and Photocatalysis Properties of Cu-Doped  $\text{TiO}_2$  Thin Films, *Applied Surface Science*. Thin Films, *Applied Surface Science* <http://dx.doi.org/10.1016/j.apsusc.2016.07.034>.

- Comert, B., Akin, N., Donmez, M., Saglam, S., and Ozcelik, S (2016). "Titanium Dioxide Thin Films as Methane Gas Sensors," *IEEE Sensors Journal*, 16, 24, 8890-8896. Doi: 10.1109/JSEN.2016.2619860.
- Dharmadasaz, I. M., and Haigh, J (2006). Strengths and Advantages of Electrodeposition as a Semiconductor Growth Technique for Applications in Microelectronic Devices *Journal of The Electrochemical Society*, 153, 1, 47-52. doi:10.1016/j.matpr.2019.06.377.
- Fasakin, O., Eleruja, M. A., Akinwunmi, O.O., Olofinjana, B., Ajenifuja., Ajayi, E.O.B (2013). Synthesis and Characterization of Metal Organic Chemical Vapour Deposited Copper Titanium Oxide (Cu-Ti-O) Thin Films from Single Solid Source Precursor *Journal of Modern Physics*, 4, 1-6 doi.org/10.4236/jmp.2013.412A3001.
- Haque, S., Mendes, M. J., Sanchez-Sobrado, O., Águas, H., Fortunato, E. and Martins, R (2019). "Photonic-structured TiO<sub>2</sub> for high-efficiency, flexible and stable
- Heiba, Z. K., Mohamed, M.B. & Badawi, A. (2022). Structural and Optical Characteristic of Cu-Doped TiO<sub>2</sub> Thin Film *Journal of Inorganic and Organometallic Polymers and Materials* 32, 2853–2862.
- Horzuma, S., Gürakarb, S., Serin, T (2019). Investigation of the Structural and Optical properties of Copper-titanium oxide thin films produced by changing the amount of copper *Thin Solid Films* 685, 293-298.
- Ijeh, R. O., Nwanya, A. C., Nkele, A.C., Madiba, I.G., Bashir, A.K.H., Ekwealor, A.B.C., Osuji, R.U., Maaza, M., Ezema, F. (2020). Optical, electrical and magnetic properties of copper doped electrodeposited MoO<sub>3</sub> thin films *Ceramics International* 46, 10820–10828.
- Ijeh, R. O., Ugwuoke, C.O., Ugwu, E. B., Aisida, S. O., Ezema, F. I. (2022). Structural, optical and magnetic properties of Cu-doped ZrO<sub>2</sub> films synthesized by electrodeposition method. *Ceramics International* 48, 4686–4692.
- karabulut, A., Dere, A., Al-sehemi, A.G., Al-Ghamdi, A. A., and Yakuphanoglu, F (2018). Cadmium Oxide: Titanium Dioxide composite Based Photosensitive Diode *Journal of Electronic Materials*, 47, 7159–7169..
- Khan, M. I., Bhatti, K. A., Qindeel, Leda, R., Bousiakoud, G., Alonizan, N (2017). Structural, Morphological, Optical and Electrical properties of 1% Cu doped TiO<sub>2</sub> multilayer nano structured thin films deposited by Sol-Gel spin coating technique *Journal of Optoelectronics and Advanced Materials* 19, 7- 8, 538 – 542.
- Kim, J., Lee, H., Na, J., Kim, S., Yo, Y., and Seong, T (2015). Dependence of Optical and Electrical Properties on Ag thickness in TiO<sub>2</sub>/Ag/TiO<sub>2</sub> multilayer films for photovoltaic devices *Ceramics International* 41, 8059–8063.
- Maziarz, W., Kusior, A., and Trenczek-Zajac, A (2017). Nanostructured TiO<sub>2</sub>-based gas sensors with enhanced sensitivity to reducing gases *Beilstein Journal of Nanotechnology*. 7, 1718–1726. doi: 10.3762/bjnano.7.164.
- Natsir, M., Maulidiyah, M., Watoni, A. H., Arif, J., Sari, A., Salim, L O A., Sarjuna, S., Irwan, I. and Nurdin, M. (2021). Synthesis and characterization of Cu-doped TiO<sub>2</sub> (Cu/TiO<sub>2</sub>) nanoparticle as antifungal phytophthora palmivora *Journal of Physics: Conference Series* doi:10.1088/1742-6596/1899/1/012039.
- Patel, S. K. S., Gajbhiye, N. S (2012). Room temperature magnetic properties of Cu-doped titanate, TiO<sub>2</sub> (B) and anatase nanorods synthesized by hydrothermal

method *Materials Chemistry and Physics* 132, 175–179.

Perarasan, T.; John Peter, I.; Muthu Kumar, A.; Rajamanickam, N.; Ramachandran, K.; Raja Mohan, C. (2019). *Copper doped titanium dioxide for enhancing the photovoltaic behavior in solar cell. Materials Today: Proceedings, S221478531931747X*–.

Sokoidanto, H., Taufik, A., and Saleh, R., (2020). Structural and optical study of Cu-doped  $TiO_2$  nanoparticles synthesized by co-precipitation method *Journal of Physics: Conference Series* 1442 012008 doi:10.1088/1742-6596/1442/1/012008.

Suber, A.S., Abdul-Hussein, K., Elttayef , Khalaf, H. K., Z.Abbas, S. , Daood, A. H (2021). Preparation of Cu-TiO<sub>2</sub> Thin Films, And Used An as Antibacterial *Journal of Physics: Conference Series* 1818 012234 IOP Publishing doi:10.1088/1742-6596/1818/1/012234.

Thangama, G. J., Devadasana, J. J., Gracea, P. S (2017). Cu Doped TiO<sub>2</sub> Thin Films Fabricated by Simple SPD Technique *IOSR Journal of Applied Physics (IOSR-JAP)* e-ISSN: 2278-4861,57-60 DOI 10.9790/4861-17002035760.

Tipparak,P., Wiranwetchayan, O., and Promnopas, W (2017). Preparation and Characterization of Copper doped Titanium dioxide thin film by sparking process *S N R U Journal of Science and Technology* 9, 3, 583-591

Vidhya, R., Sankareswari, M., Neyvasagam, K (2016). Effect of annealing temperature on structural and optical properties of Cu-TiO<sub>2</sub> thin film *International Journal of Technical Research and Applications* 37, 42-46.

Zeribi, F., Attaf, A., Derbali, A., Saidi, H., Benmebrouk, L., Aida, M. S., Dahnoun, M., Nouadji, R., and Ezzaouia, H (2022). Dependence of the Physical

Properties of Titanium Dioxide (TiO<sub>2</sub>) Thin Films Grown by Sol-Gel (Spin-Coating) Process on Thickness *The Electrochemical Society Journal of Solid State Science and Technology* 2022 11 023003 DOI: 10.1149/2162-8777/ac5168.

Zhang, W., Li, Y., Zhu, S., Wang, F (2004). Copper doping in titanium oxide catalyst film prepared by dc reactive magnetron sputtering *Catalysis Today*, 93, 95, 589–594.